

## TIDAL PERIODICITIES IN OBSERVATIONS OF THE OH(6–2) EMISSION FROM EASTERN ANTARCTICA.

Greet P.A.<sup>1</sup>, Murphy D.J.<sup>1</sup>, and Dyson P.L.<sup>2</sup>

1: Australian Antarctic Division, Channel Highway, Kingston, Tasmania 7050.

2: Department of Physics, La Trobe University, Bundoora, Victoria 3083.

### ABSTRACT

High-resolution Fabry-Perot spectrometer observations of the OH (6–2) Q<sub>1</sub>(1) line,  $\lambda 834.460$  nm, were made at Mawson, 67.6°S 62.9°E, and Davis, 68.6°S 78.0°E, Antarctica, in 1997. The observing program resulted in three sets of continuous OH observations suitable for tidal analysis: July 25<sup>th</sup> – 31<sup>st</sup> when the Mawson FPS observed for 7 days, and August 3–7<sup>th</sup> and 10–14<sup>th</sup> when the Davis FPS observed for two five day intervals. Lomb-Scargle periodograms show a definitive 12 hour periodicity in the meridional and zonal winds at both stations. The OH emission intensity has a dominant 24 hour periodicity which may be either tidal or photochemical in nature. Superposed epoch analysis is used to determine amplitude and phase of the 12- and 24-hour periodicities. At these latitudes the semidiurnal tide is dominant with amplitude of 10–30 ms<sup>-1</sup> while the diurnal tide has amplitudes of only 0–5 ms<sup>-1</sup>. Comparison is made with MF radar measurements. Simultaneous measurements from a radar at Davis compare well with FPS measurements; amplitudes and phases agree and both instruments measure a larger amplitude for the semi-diurnal tide in the last two weeks of July than in the first two weeks of August.

### X.1 INTRODUCTION

The middle atmosphere is highly variable. Instantaneous measurements of winds, temperature, density, or airglow emission intensity can vary significantly from the mean due to wave or tidal perturbations. The amplitude and phase of waves and tides vary and considerable effort has been made to build tidal models for the mesosphere and lower thermosphere (e.g. Forbes, 1982; Forbes *et al.*, 1997; Yudin *et al.*, 1997). To model the tides properly it is necessary to know the typical tidal variations, the range of variation likely, and ideally the cause of large tidal variations. This requires much data, from a number of techniques, over a period of time. WINDII and HRDI experiments aboard the UARS satellite have provided data on mesosphere and lower thermosphere tides (e.g. McLandress *et al.*, 1996; Palo *et al.*, 1997). However sampling between 40 and 60 degrees latitude is limited and no sampling occurs above 60 degrees latitude. Tidal observations above 60 degrees are thus of particular interest.

Mesospheric tides are global in nature and specific modes dominate in particular circumstances (Forbes, 1982). At low- and mid-latitudes migrating tidal modes dominate. These modes have either zero or small amplitudes at high-latitudes. Observations at high latitudes indicate the presence of large-scale waves and non-migrating tides (Palo *et al.*, 1998; Sivjee and Walterscheid, 1994; Hernandez *et al.*, 1995 & 1996). Mawson and Davis are at latitudes still affected by migrating tides (Forbes, 1982; Phillips and Vincent, 1989; Greet and Dyson, 1999). It is possible that several tidal modes may be present simultaneously.

Tides are an important part of mesospheric dynamics and knowledge of their behaviour is necessary, for example, if effects of long-term climate change are to be detected. Systematic bias due to changes in tidal amplitude or phase, inherent in the data sampling, must be allowed for or considered.

This paper presents Fabry-Perot spectrometer observations of the OH (6–2) Q<sub>1</sub>(1) line at  $\lambda$ 834.5 nm. Observations of this emission commenced at Mawson in 1993 (Greet *et al.*, 1994). A subsequent campaign in 1995 revealed semidiurnal tidal periodicities in winds and intensities (Greet and Dyson, 1999). Further OH observations from Mawson, 67.6°S 62.9°E, and Davis, 68.6°S 78.0°E, in 1997 also contain tidal periodicities as discussed in the following sections.

## X.2 INSTRUMENTS AND DATA

The Mawson Fabry-Perot spectrometer is described in detail by Jacka (1984). A similar instrument, originally operated at Mt Torrens in the Adelaide hills (Jacka *et al.* 1980, Cocks *et al.* 1980), has been adapted for dual-channel, single-etalon operation and installed at Davis. Routine observations at Davis commenced in 1997. OH observing campaigns are co-ordinated between the two stations. Greet *et al.* (1994) describe the technique used to determine the relative intensity of the OH nightglow emission, and mesospheric winds and temperature variations from FPS observations of the (6–2) Q<sub>1</sub>(1) line at  $\lambda$ 834.5 nm.

In 1997 an OH campaign was scheduled for the month of July at Mawson. With the dual-channel operation at Davis, OH observations were scheduled for a longer interval, the month of July and continuing until mid-August. For FPS OH observations to be carried out the weather must be fine and the sky mostly clear. At times observations are made through thin cloud but if cloud thickened or there was any chance of snow, observations ceased. This paper will look in detail at three intervals: July 25<sup>th</sup> – 31<sup>st</sup> when the Mawson FPS observed for seven days, and August 3–7<sup>th</sup> and 10–14<sup>th</sup> when the Davis FPS observed for two five-day intervals. In 1997 weather conditions did not permit the two stations to observe simultaneously for more than two consecutive days.

To extract tidal information from highly variable mesospheric measurements a number of days of data are required. Tides vary in phase and amplitude and analysis techniques assume the phase and amplitude are constant. This is reasonable for periods of about 10 days. Optical observations are limited to dark skies and hence data are available for considerably less than 24 hours a day, at all but the highest latitudes. Even so tidal variations are obvious in mesospheric observations but care must be taken to consider aliasing effects of optical sampling.

Palo *et al.* (1997) discuss the effects of aliasing on sampled data. Aliasing masks, similar to those in Figure 2 of Palo *et al.*, were generated for the 1997 FPS OH campaigns. The masks are Fourier transforms of step functions to select data samples from a uniformly sampled population. The mask for meridional samples of the Davis August 10–14<sup>th</sup> campaign is shown in Figure 1. All masks had similar characteristics with substantial power at 1 cycle per day, and further less-significant power peaks at multiples of 1 cycle. Palo *et al.* (1997) note that this can cause leakage of power from 24 hours into the mean, from the mean and 12 hours into the diurnal tide and from 24 and 8 hours into the semidiurnal tide.

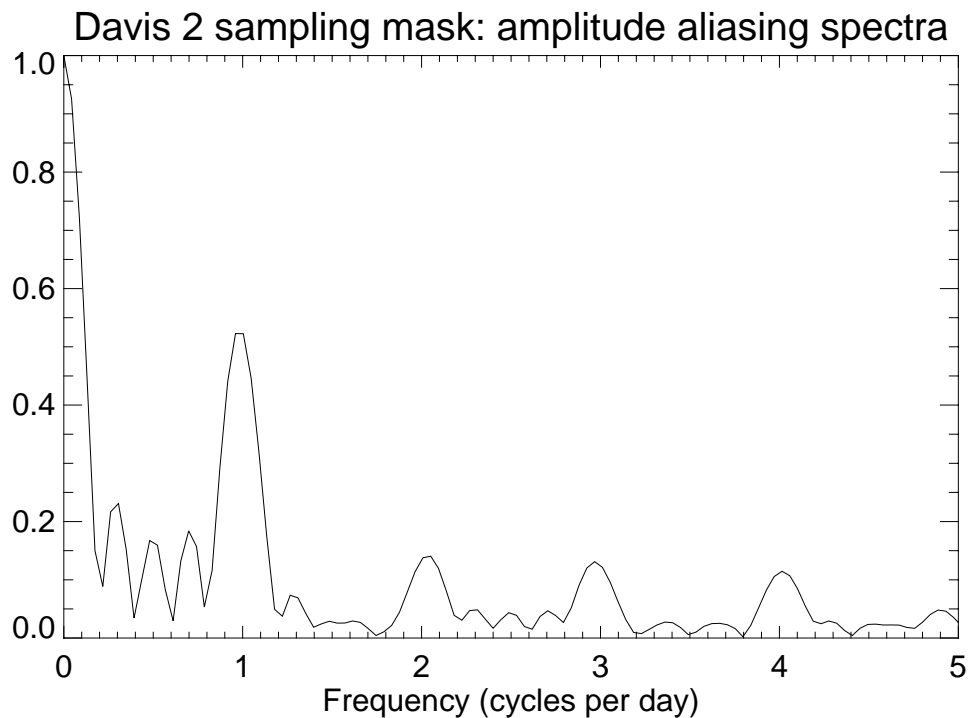


Figure 1: Aliasing spectrum from meridional samples during the Davis campaign 10–14<sup>th</sup> August, 1997. Significant power occurs at 1 cycle per day, and some power at 2, 3, and 4 cycles per day.

In 1995, an OH observing campaign at Mawson obtained 14 days data in a 15 day interval. This has been analysed by Greet and Dyson (1999). In this data it was possible, using Lomb-Scargle periodograms, to identify the semi-diurnal tide in the meridional wind data. A Lomb-Scargle periodogram of raw data was performed, followed by a second periodogram of the raw data minus a 12 or 24 hour fit. Simulations showed that if the wrong periodicity were subtracted from the data, power at 8 hours would remain in the periodogram. This type of analysis for the 1997 campaigns will be presented in the next section.

No significant periodicities were present in temperature measurements from the 1995 campaign and none were found in any of the three 1997 campaigns. This does not imply that no temperature periodicities are present merely that any temperature variation is less than  $\sim 11$  K, approximately half the mean uncertainty in the temperature measurements (Greet and Dyson, 1999). Temperature measurements will not be included in the following discussion.

### X.3 LOMB-SCARGLE ANALYSIS

Figure 2 shows Lomb-Scargle periodograms of the OH emission intensity and wind, for meridional and zonal measurements from the Mawson campaign, July 25<sup>th</sup>–31<sup>st</sup>, 1997. Each of the seven days in this interval had 14–15 hours of data. Periodograms of the raw data, [a] or column 1 of figure 2, show that  $11.9 \pm 0.5$  hour is the most significant periodicity in the meridional and zonal wind, although it is not statistically significant in the meridional wind. There is no significant power at 24 hours in either the meridional or zonal wind. In the zonal wind, subtraction of a fitted 12-hour periodicity, column [c], leaves no significant periodicities and subtraction of a fitted

24-hour periodicity, column [d], leaves some power at 8 hour, albeit only at a 50% significance level. This is evidence of a 12-hour periodicity in the wind.

In both the meridional and zonal emission intensity the most significant periodicity is near 24 hours. There is some power at 12 hours in the meridional emission intensity but it is not significant, and in the zonal intensity the power at 12 hours is near the noise level. Subtracting a fitted 12-hour periodicity leaves power at 8 hours, again not reaching the 95% significance level. Subtracting a 24-hour periodicity leaves power only at longer periodicities. This is evidence of a 24-hour periodicity in the intensity.

OH emission intensity may show periodicities from photochemical as well as tidal sources.

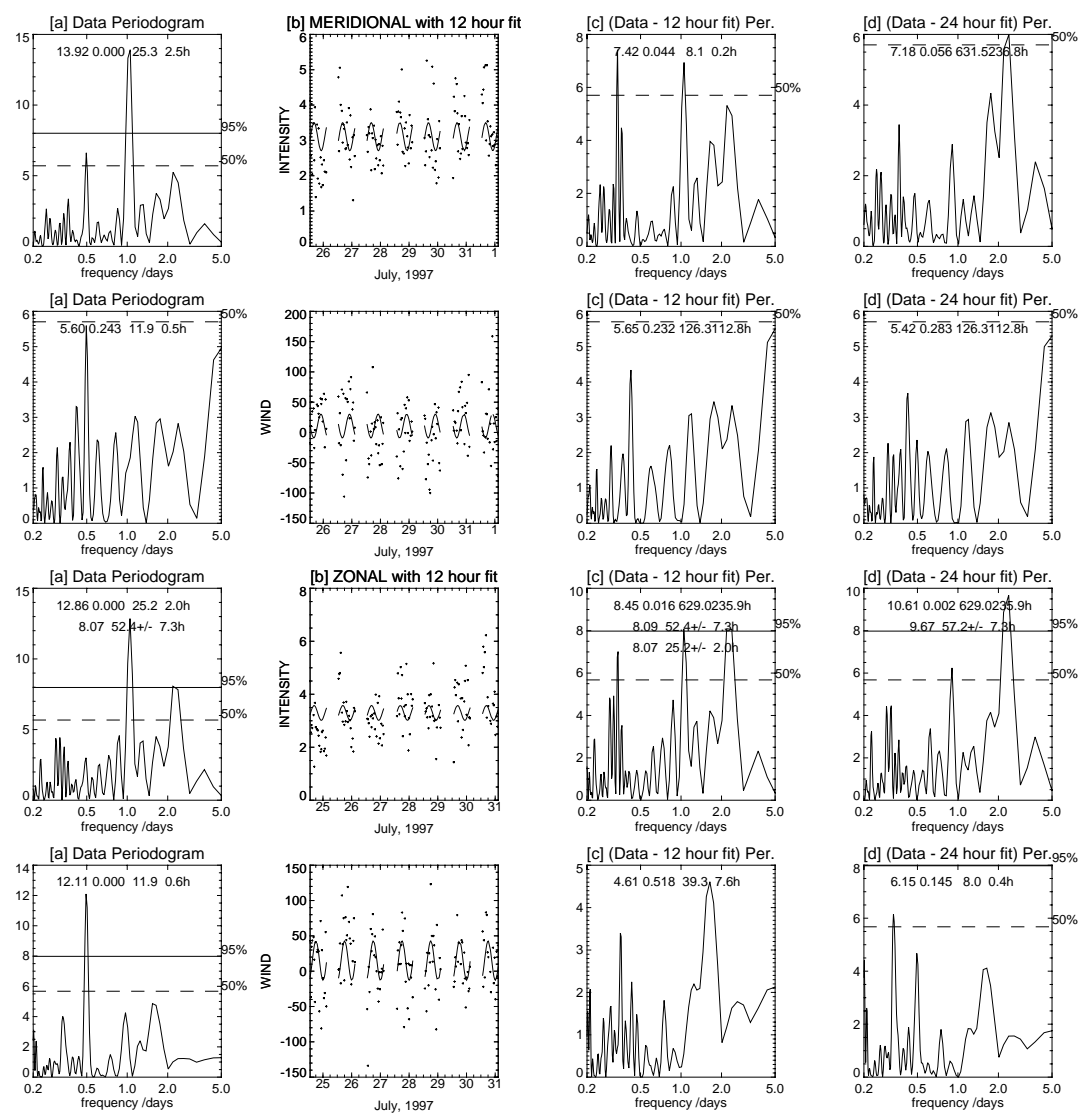


Figure 2 : Lomb-Scargle periodograms of meridional emission intensity and wind, and zonal emission intensity and wind for the Mawson campaign, July 25<sup>th</sup>–31<sup>st</sup>, 1997. [a] periodogram of data, [b] data with 12 hour fit subtracted, [c] periodogram of data with 12 hour fit subtracted, and [d] periodogram of data with 24 hour fit subtracted. After subtraction of a fitted component, residual power at 8 hours indicates an inappropriate fit to the data.

Intensity measurements during the Davis campaign from 3–7<sup>th</sup> August, 1997, are dominated by tropospheric cloud which generated a 2.5 day periodicity. There was significant power at  $21 \pm 1$  hours in the meridional and zonal emission intensity but no significant power at or near 12 hours. In the meridional (zonal) wind,  $11 \pm 1$  ( $11.6 \pm 0.6$ ) hours was the most significant periodicity;  $23 \pm 2$  was also significant in the zonal wind. Subtraction of fitted 12- or 24-hour periodicities did not distinguish between them. Periodicities from this interval are slightly less, although not always significantly less, than theoretical tidal periodicities of 12 and 24 hours.

The Davis campaign from 10–14<sup>th</sup> August, 1997 also had significant power at  $22 \pm 1$  hours in the zonal and meridional emission intensity. Power at 12 hours was significant at the 50% level in the meridional emission intensity, and almost so in the zonal emission intensity. In the meridional wind 12 hours was the most significant periodicity and  $26 \pm 3$  hours was also significant. In the zonal wind 12 hours was the most significant periodicity, but not quite reaching the 95% level of significance. Subtracting 12 and 24 hour fitted periodicities did not provide evidence for one periodicity over another. This is possibly due to a contribution from both 12 and 24 hours, with 12 hours being dominant in the wind and 24 hours being dominant in intensity variations.

Power at a given periodicity does not necessarily imply the presence of a tidal oscillation. If the phases of meridional and zonal periodicities are in agreement with that predicted by models then we have more confidence in a tidal interpretation. Attempts to obtain amplitude and phase information from simultaneous fitting of 12- and 24-hour periodicities will now be discussed.

#### **X.4 SUPERPOSED EPOCH ANALYSIS**

Previous studies at Mawson (Vincent, 1994) suggest that, at this time of year, the semidiurnal tide is dominant and the contribution of the diurnal tide is small. Interannual variability shows that at times the diurnal tidal contribution may be significant. Lomb-Scargle analysis suggests that, for the intensity at least, diurnal variations are significant or dominant. Greet and Dyson (1999) only fitted either 12- or 24-hour components to the data. If both 12- and 24-hour components are present then ideally they should be fitted simultaneously.

Fitting tidal components to the data also suffers from the effects of aliasing. The Lomb-Scargle analysis used a simple IDL curve-fitting routine, CURVEFIT, to subtract the mean plus 12- or 24-hour components. This will be called a two component fit. This was extended and a more robust curve fitting routine, SVDFIT, was also used to fit a mean, 12- and 24-hour (three) components. Both of these routines gave problems, with power from the mean leaking into the 24-hour component being the most common fault. This is obvious comparing a two component, three parameter, fit and the three component, five parameter, fit. Anomalously low, or high, mean value and high diurnal value are returned by the latter.

Large point-to-point variability hinders fitting tidal components. High frequency variability is common to most mesospheric measurements. A super-posed epoch analysis eliminates, or at least minimises, high-frequency variability. Figure 3 shows the analysis for the combined Davis meridional and zonal winds. In the combined

Davis data set, 10 of 12 days in the interval 3–14 August are sampled. Column (a) contains periodograms; (b) superposed epoch analysis fitting mean and combined 12- and 24-hour; and (c) as for (b) but only fitting mean and 12-hour components. Because of the complexity of the intensity spectra, the dominance of 24-hour rather than 12-hour components, with photochemical and tidal effects present, the following analysis deals only with wind measurements.

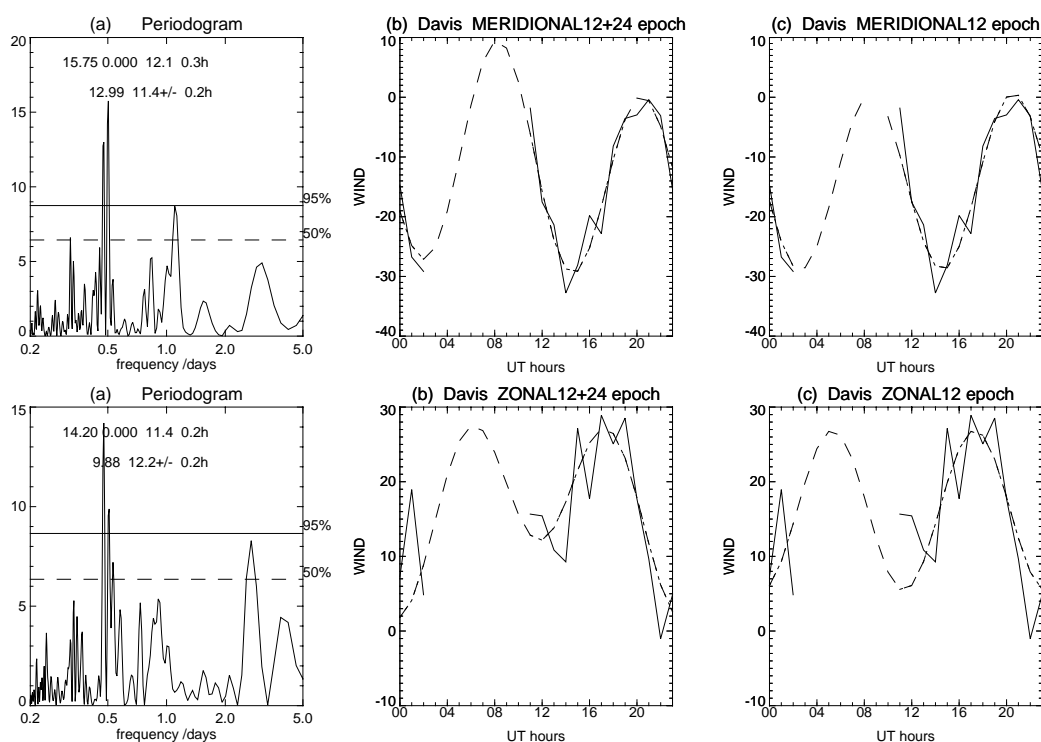


**Figure 3:** Superposed epoch analysis of the combined Davis wind meridional (top) and zonal (bottom) data sets, 10 days of data in the 12 day period 3–14<sup>th</sup> August, 1997. (a) periodograms, (b) superposed epoch data, and 5 component mean, 12 and 24 hour fit (dashed curve) (c) as for (b) but three component mean and 12 hour fit.

The periodograms show two significant frequencies, 12.1 and 11.4 hours, in both the meridional and zonal wind. The aliasing mask for the zonal data from the combined Davis campaigns, in Figure 4, shows high frequency structure which would produce this splitting of the power at 12 hours. The power at 2.12 cycles per day is larger in the zonal than meridional, 0.65 as compared to 0.45, which would explain the difference in the Lomb values for the two data sets.

The fitted diurnal component is small. There is reasonable agreement between the fitted mean and 12-hour components from both the 2 and 3 component fits for both the meridional and zonal data. Table 1 gives the fitted parameters for Davis and Mawson data. Fitted values are grey if a poor fit was noted on visual assessment. Other discrepancies are obvious when comparing the two fits, in particular, the amplitude of the 12- and 24-hour oscillations in the Davis 2 meridional data set, and Mawson zonal data set. In both cases aliasing is skewing the results and they have also been colour-coded grey.

### Zonal sampling mask for combined Davis campaigns: amplitude aliasing spectra

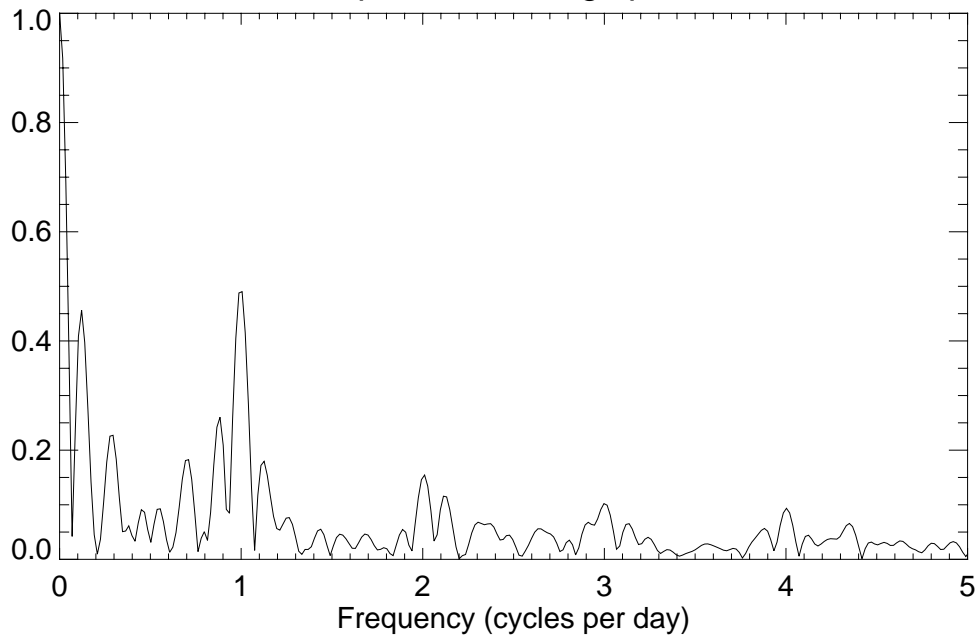


Figure 4: Aliasing spectrum from zonal samples during the combined Davis campaign 3<sup>rd</sup>–14<sup>th</sup> August, 1997. The small scale structure producing peaks at both 2.0 and 2.12 cycles splits the power at 12 hours in the data into two periodicities, as seen in Figure 3. Note differences from Figure 1.

Allowing for the diurnal component by fitting five parameters is of limited success. The amplitude and phase of the 12-hour component is in reasonable agreement between the two fits. Figure 5 shows superposed epoch analysis for the Mawson campaign. Expanding the data set to include partial days and isolated nearby days did not significantly alter the result.

**Table 1: Fitted amplitudes, in  $\text{ms}^{-1}$ , and phases, in h UT, for ZONAL wind, various campaigns.**

		$n_{\text{days}}$	$A_0$	$A_{12}$	$\Phi_{12}$	$A_{24}$	$\Phi_{24}$		$A_0$	$A_{12}$	$\Phi_{12}$
Davis	3–14 Aug	10 in 12	17	10	6	5	12		16	11	5
Davis 1	3–7 Aug	5 in 5	17	5	3	9	13		17	8	4
Davis 2	10–14 Aug	5 in 5	14	14	6	2	22		15	15	6
Mawson	25–31 Jul	7 in 7	0	25	5	31	20		16	27	6

**Table 2: As for Table 1, but for MERIDIONAL wind.**

		$n_{\text{days}}$	$A_0$	$A_{12}$	$\Phi_{12}$	$A_{24}$	$\Phi_{24}$		$A_0$	$A_{12}$	$\Phi_{12}$
Davis	3–14 Aug	10 in 12	-12	17	8	5	7		-14	15	9
Davis 1	3–7 Aug	5 in 5	-14	17	8	8	8		-18	13	8
Davis 2	10–14 Aug	5 in 5	-8	40	9	19	11		-11	50	9
Mawson	25–31 Jul	7 in 7	15	22	10	11	8		11	27	10

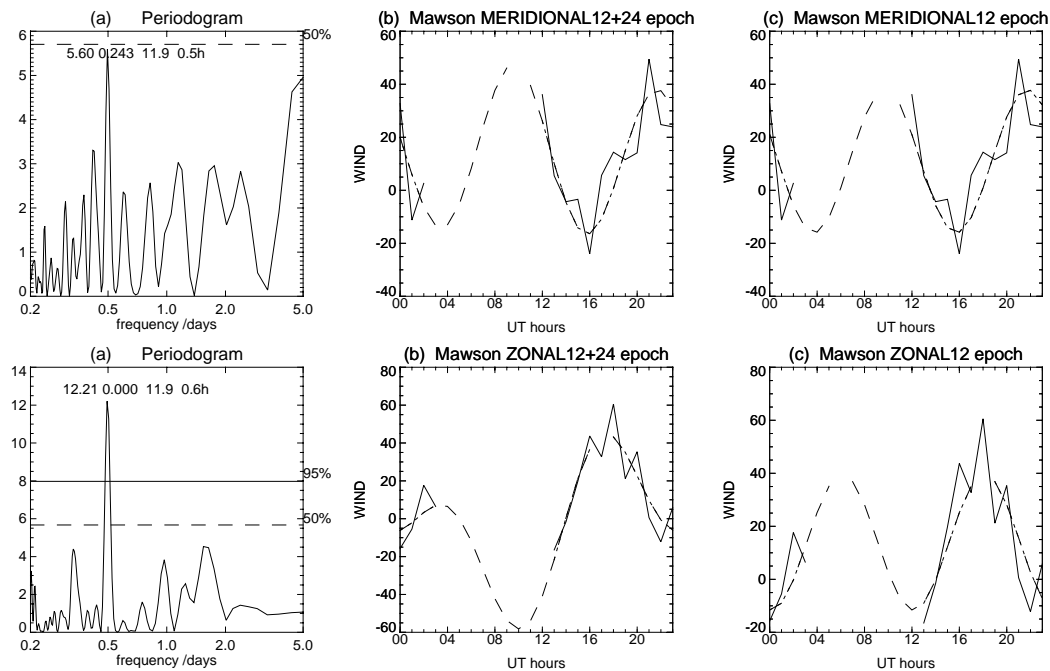


**Figure 5:** Superposed epoch analysis of the Mawson wind meridional (top) and zonal (bottom) data sets, from 25<sup>th</sup>–31<sup>st</sup> July, 1997. (a) periodograms, (b) superposed epoch data, and 5 component mean, 12 and 24 hour fit (dashed curve) (c) as for (b) but three component mean and 12 hour fit.

## X.5 DISCUSSION

### x.5.1 High-Latitude Semidiurnal Tide

The fitted 12 hour component is significantly larger than the 24-hour component. Figure 3 and tables 1 and 2, show that for the fitted 12-hour component the zonal wind phase leads the meridional by approximately  $\pi/2$ , 3 hours, as expected for the migrating tide in the southern hemisphere.

*‘During April, May, July, and August the phases at Scott Base, Molodezhnaya, and Mawson are within about 1 h of 0100 LT; a constant phase with respect to longitude is consistent with a semidiurnal oscillation migrating with the apparent motion of the sun.’* Portnyagin *et al.* (1998) note when comparing the 12-hour oscillation, from radar observations, at South Pole, Scott Base, Molodezhnaya and Mawson. The phase referred to here is that of the meridional component. From the 2 component fit in Figure 3 the Davis meridional 12-hour component maximises near 08 UT, which is 01 LT to within 15 minutes. From similar plots for Mawson, Figure 5, the meridional 12-hour component maximises near 10 UT, which is 02 LT to within 15 minutes. These values for Mawson and Davis are not from simultaneous data sets. A superposed epoch analysis was performed on data obtained simultaneously at Davis, the Davis FPS observed for 8 of the 14 days from July 19<sup>th</sup>–August 1<sup>st</sup>, but there were insufficient data to well fit amplitude and phase parameters.

To better compare phases between Mawson and Davis we need to split the data sets into individual directions as Mawson east and Davis west viewing volumes are adjacent to each other compared to the distances between east and west viewing volumes for one individual station. This was done but with marginal success because of poor signal to noise. Values obtained from the superposed epoch fit for all Davis and Mawson data in individual directions show that the amplitude of the 12-hour component maximises in the Davis east viewing volume, approximately 2 hours prior to the Mawson west viewing volume. These two volumes are separated by 30 degrees

of latitude. Rigorous uncertainty calculations have not been included and considering the limited number of points this result should be considered qualitatively rather than quantitatively. That the Davis east volume phase is in advance of the Mawson phase is further evidence for interpretation of the 12-hour oscillation as the migrating semidiurnal tide.

This discussion of the semi-diurnal tide has been restricted to oscillations in the wind. It is hoped that by comparison with models we can extend our analysis to include OH emission intensity. At present an approximately 24-hour periodicity dominates in the OH emission intensity. There is some power at 12 hours but aliasing and the presence of both photochemical and tidal variations make interpretation of the OH emission intensity data beyond the scope of this work.

#### *X.5.2 Comparison with Mawson radar winds*

An MF radar was operational at Mawson from 1981–93 and data are readily available for the years 1984–90 (Vincent, 1994). The radar was upgraded and moved to Davis in 1994 and was operational during 1997. The radar samples every two kilometres with a four kilometre range resolution.

The OH emission originates from a layer of approximately 7 km half width at a height of 87 km (Baker and Stair, 1988). The layer shape varies significantly with large tidal and wave perturbations in the region. FPS observations integrate the OH emission over the entire layer. By ignoring possible complexities in the OH layer shape a simple comparison can be made between the FPS OH observations and a single radar height near the peak of the OH layer. We have chosen a radar height of 86 km for such a comparison.

Spatial variations also potentially affect measurements from two instruments. The radar beam was 40 degree half-width half-maximum. This corresponds to a field of view of approximately 150 km at an altitude of 87 km. The radar beam pointed to the zenith. The FPS semi-angle field of view was 13 mrad. This corresponds, at a 75 degree zenith angle, to a column through the OH layer approximately 40 km in diameter. The meridional and zonal FPS viewing volumes are separated by 650 km. Thus the two instruments spatially average in quite different ways.

Meridional and zonal winds from the FPSs, the MF radar and a model are compared in Tables 3 and 4. These tables are expansions of Tables 1 and 2 to include: simultaneous MF radar data from Davis for the specific intervals of the FPS campaigns; 12 day radar averages from Mawson for the years 1984–90 (Vincent, 1994); and GSWM-98 model values for a height of 86 km and latitudes -66 and -69 (Hagan *et al.*, 1999; <http://www.hao.ucar.edu/public/research/tiso/gswm/gswm.html>). The values in square brackets next to the Mawson radar averages are the standard deviations indicative of typical variations in the mean.

The Mawson FPS mean and semi-diurnal tidal amplitudes are significantly larger than the average Mawson MF radar values. The Mawson radar values are averaged over seven years and, although an indication of variability is available, the value obtained on any given year may differ substantially. Considering the spatial differences in the two sampling techniques it is probably still useful to also compare the Mawson FPS amplitudes with those obtained simultaneously by the Davis radar. Theoretically the

phase of the tide at Mawson should lag that at Davis by 1 hour. We will first consider the diurnal and then the semidiurnal tides.

**Table 3: Fitted amplitudes,  $\text{ms}^{-1}$ , and phases, in hour UT, for ZONAL wind, various campaigns.**

		$n_{\text{days}}$	$A_0$	$A_{12}$	$\Phi_{12}$	$A_{24}$	$\Phi_{24}$	$A_0$	$A_{12}$	$\Phi_{12}$
Mawson	25–31 Jul	7 in 7	0	25	5	31	20	16	27	6
Davis	3–14 Aug	10 in 12	17	10	6	5	12	16	11	5
Davis 1	3–7 Aug	5 in 5	17	5	3	9	13	17	8	4
Davis 2	10–14 Aug	5 in 5	14	14	6	2	22	15	15	6
Davis	25-31 Jul	Radar	6	18	6	1	7			
	3–14 Aug	Radar	16	10	6	1	12			
	3–7 Aug	Radar	29	11	6	4	5			
	10–14 Aug	Radar	10	14	6	5	16			
Mawson	204, 84–90	Radar	10[6]	9 [3]	7 [5]	7 [7]	9 [6]			
	216, 84–90	Radar	8 [8]	9 [5]	5 [6]	5 [3]	11[6]			
	228, 84–90	Radar	11[8]	9 [5]	9 [5]	4 [3]	12[7]			
GSWM	July solstice	Lat $-66^\circ$		22.7	12.1	4.1	18.3			
		Lat $-69^\circ$		20.3	12.2	6.6	17.7			

**Table 4: As for Table 3 but for MERIDIONAL wind, various campaigns.**

		$n_{\text{days}}$	$A_0$	$A_{12}$	$\Phi_{12}$	$A_{24}$	$\Phi_{24}$	$A_0$	$A_{12}$	$\Phi_{12}$
Mawson	25–31 Jul	7 in 7	15	22	10	11	8	11	27	10
Davis	3–14 Aug	10 in 12	-12	17	8	5	7	-14	15	9
Davis 1	3–7 Aug	5 in 5	-14	17	8	8	8	-18	13	8
Davis 2	10–14 Aug	5 in 5	-8	40	9	19	11	-11	50	9
Davis	25-31 Jul	Radar	-6	19	8	5	4			
	3–14 Aug	Radar	-10	12	8	3	3			
	3–7 Aug	Radar	-12	13	8	2	4			
	10–14 Aug	Radar	-8	17	8	3	1			
Mawson	204, 84–90	Radar	3 [4]	10[5]	5 [4]	6 [4]	9 [9]			
	216, 84–90	Radar	3 [4]	11[6]	4 [4]	5 [4]	9 [6]			
	228, 84–90	Radar	-1 [5]	12[7]	3 [2]	7 [7]	10[9]			
GSWM	July solstice	Lat $-66^\circ$		23.4	3.1	5.7	0.1			
		Lat $-69^\circ$		21.8	3.1	5.5	0.2			

The fitted 24-hour component in both the FPS and radar winds is small, of the order of  $5 \text{ ms}^{-1}$  or less. It is difficult for the FPS to well determine the amplitude and phase of such a small contribution considering the inherent optical sampling difficulties and general mesospheric variability. Meridional and zonal amplitude and zonal phase values obtained from the 3 component fit are in reasonable agreement with those of MF radar and the GSWM model. Diurnal variations in OH emission intensity are larger and hence probably photochemical in origin.

The amplitude of the semi-diurnal tide is also more similar in the FPS and simultaneous Davis radar than the averaged Mawson radar amplitudes. The FPS 12-hour amplitudes are slightly larger than the Davis radar amplitudes possibly because of the smaller FPS sampling volumes. Differences between the radar and FPS semidiurnal amplitudes are also associated with differences in the fitted mean winds.

There is good agreement between the general trends in the FPS and radar mean and 12-hour components. Both the simultaneous Davis radar and the FPS measurements indicate that the amplitude of the 12-hour component is larger in the last two weeks of July than in August. The mean zonal and meridional winds vary in a similar fashion between the Davis radar and FPS observations, although the Mawson FPS means are somewhat different.

The well fitted zonal FPS mean and 12-hour components are in good agreement, both between the 2 and 3 component FPS fits and the FPS and radar fits. For the meridional winds, the 2 and 3 component FPS fits vary more and the agreement between the FPS and simultaneous Davis radar values is not as good as for the zonal winds. This may be due to variability in the tide and/or the presence of other perturbations in the wind field which makes the tides difficult to isolate. Figures 6 and 7 show the Davis radar measured meridional and zonal winds for the Mawson and combined Davis campaigns. The continuous radar sampling allows easier visual identification of tidal variations. The smooth overlaid curve is the combined, mean, 12- and 24-hour fit.

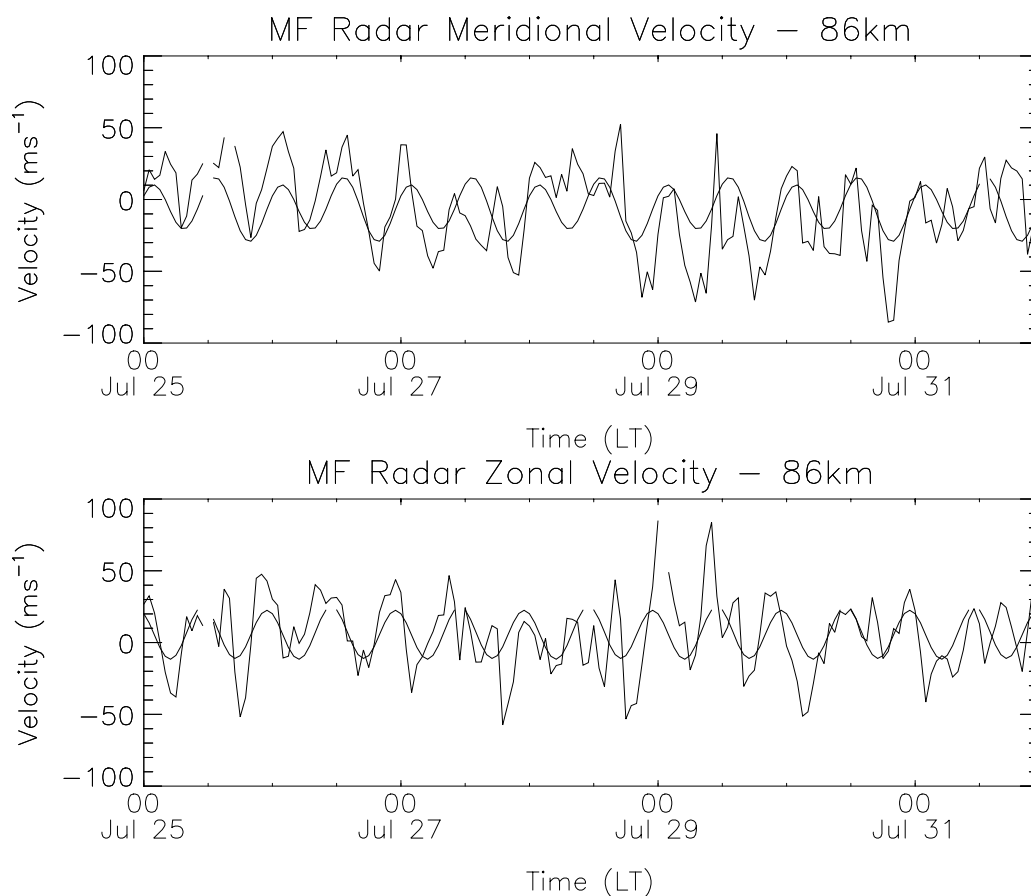


Figure 6: Davis MF radar meridional and zonal winds obtained during 25-31 July when the Mawson FPS was observing. The smooth overlaid curve is the combined mean, 12- and 24-hour fitted components.

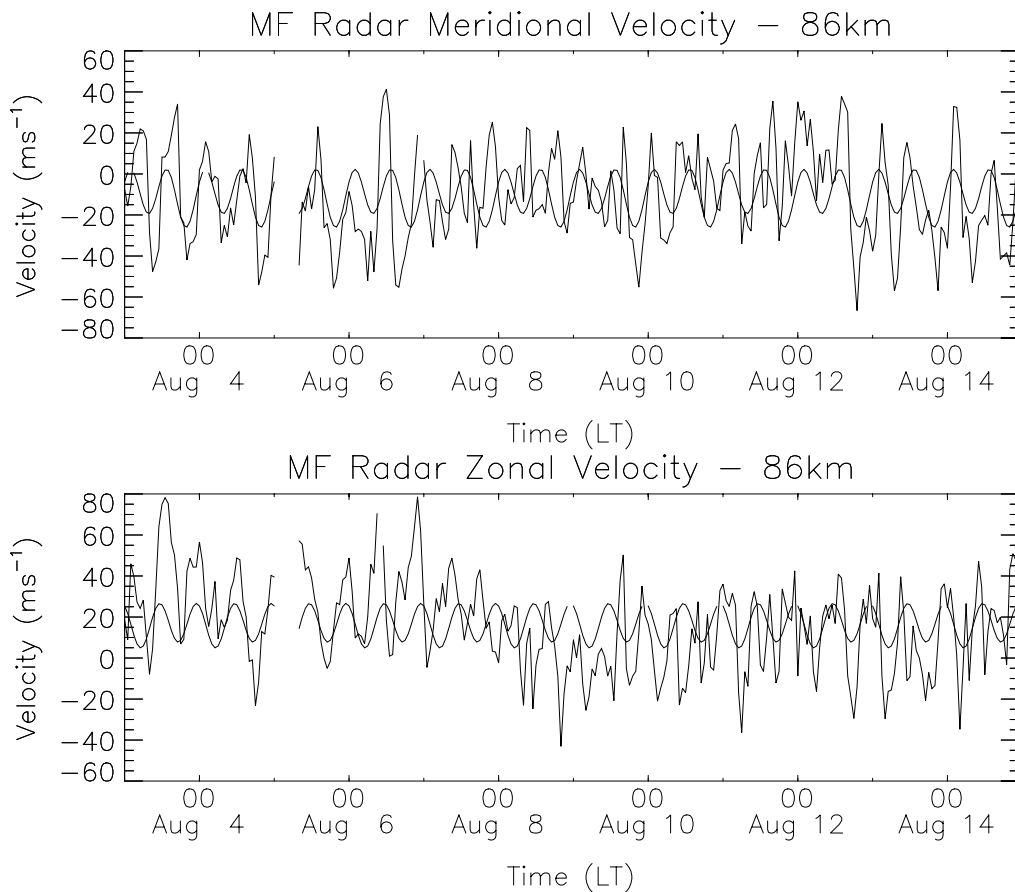


Figure 7: Davis MF radar meridional and zonal winds obtained during 3-14 August, 1997. This coincides with the two Davis FPS campaigns. The smooth overlaid curve is the combined mean, 12- and 24-hour fitted components.

### X.5.3 Comparison with other southern polar wind studies

Hernandez *et al.* (1995) looked at periodicities in FPS OH observations at South Pole and MF radar at Scott Base identifying 10-hour and 2-day periodicities in Scott Base and South Pole data, as well as 7-, 12- and 24-hours at Scott Base. South Pole data were used to identify the oscillations as zonal wavenumber one waves. Portnyagin *et al.* (1998) have studied in detail periodicities in meteor wind data from South Pole over a year. They note the dominance of 12- and 24-hour periodicities in summer and from April to October the dominance of oscillations with periods less than 12 hours and periods from 2–10 days. Sivjee and Walterscheid (1994) identified temperature oscillations of six hours in OH emission brightness and rotational temperature measurements at South Pole. We note that in FPS wind measurements from Mawson and Davis there are no significant periodicities other than 12 hours.

## X.6 CONCLUSIONS

FPS observations of the OH emission have been made at Mawson and Davis during 1997. Lomb-Scargle periodograms have been used to identify a 12-hour periodicity in the wind. A superposed epoch analysis has been used to fit mean, 12- and 24-hour components to the data. As the zonal phase of the 12-hour component leads the meridional phase by 3 hours, and the phase at Davis leads that at Mawson, and in both cases maximises at approximately 0100LT, we identify this oscillation as the

migrating semi-diurnal tide. Fitted amplitudes of the diurnal tide are of the order of or less than  $5 \text{ ms}^{-1}$ . The amplitude of the semidiurnal tide varies between 10 and  $30 \text{ ms}^{-1}$  over the campaigns.

Comparisons have been made between the FPS and MF radar measurements. Averaged radar tides from seven years of data at Mawson imply smaller values than were seen by the FPS. Simultaneous data obtained with the MF radar at Davis were in good agreement with the FPS measurements. Both instruments measured larger,  $20\text{--}30 \text{ ms}^{-1}$ , semi-diurnal tides in the last two weeks of July than in August when the amplitudes were in the range  $10\text{--}15 \text{ ms}^{-1}$ . Differences between the two instruments may be due to the different spatial averaging or different fitting routines. The times when differences between the two techniques were largest coincided with the times when the tides were less obvious or more variable.

The only frequencies positively identified in this study are those at 12 and 24 hours. There is no indication of the presence of 10-hour oscillations in the three 1997 campaigns.

Further OH observing campaigns have been carried out and it is hoped that the FPS radar comparison can be extended to larger data sets and times when the Mawson and Davis FPSs obtained simultaneous data.

## **X.7 ACKNOWLEDGEMENTS**

We acknowledge support by the Australian National Antarctic Research Expeditions, the Australian Antarctic Science Advisory Committee, and the Australian Research Council. Mr Chris Boucher collected the 1997 Mawson FPS data and Mr Mike Manion assisted with the Davis FPS and ran the Davis radar in 1997. General support from other expeditioners through the year was appreciated. Dr R.A. Vincent, University of Adelaide, supplied the Mawson radar tidal data. Thanks to M. Hagan and associates for free, easy web access to the GSWM-98 results at the site: <http://www.hao.ucar.edu/public/research/tiso/gswm/gswm.html>.

## **X.8 REFERENCES**

- Baker D.J. and Stair A.T. (1988). Rocket Measurements of the Altitude Distributions of the Hydroxyl Airglow. *Phys. Scripta* 37: 611–622.
- Cocks T.D., Creighton D.F., and Jacka F. (1980). Application of a dual Fabry-Perot spectrometer for daytime airglow studies. *Journal of Atmospheric and Terrestrial Physics* 42: 499–511.
- Forbes J.M. (1982). Atmospheric tides 2. The solar and lunar semidiurnal components. *Journal of Geophysical Research* 87: 5241–5252.
- Forbes J.M., Hagan M.E., Zhang X., Hamilton K. (1997). Upper Atmosphere Tidal Oscillations due to Latent Heat Release in the Tropical Troposphere. *Annales Geophysicae* 15: 1165–1175.
- Greet P.A. and Dyson P.L. (1999). Tidal Periodicities in Observations of the OH(6–2) Emission from Mawson, Antarctica. *Advances in Space Research* (in press).

Greet P.A., Innis J. and Dyson P.L. (1994). High resolution Fabry-Perot observations of mesospheric OH (6–2) emissions. *Geophysical Research Letters* 21: 1153–1156.

Hagan, M.E., Burrage M.D., Forbes, J.M., Hackney, J., Randel W.J., Zhang X. (1999) GSWM-98: Results for migrating solar tides. *Journal of Geophysical Research* 104: 6813–6828.

Hernandez G., Smith R.W., and Fraser G.J. (1995). Antarctic High-latitude Mesospheric Dynamics. *Advances in Space Research* 16(5): 71–80.

Hernandez G., Forbes J.M., Smith R.W., Portnyagin Y., Booth J.F., and Makarov N. (1996). Simultaneous mesospheric wind measurements near South Pole by optical and meteor radar methods. *Geophysical Research Letters* 23: 1079–1082.

Jacka F. (1984). Application of Fabry-Perot spectrometers for measurement of upper atmosphere temperatures and winds. in *Middle Atmosphere Program* ed. R. Vincent 13: 19–40.

Jacka F., Bower A.R.D., Creighton D.F., Wilksch P.A. (1980). A large-aperture high-resolution Fabry-Perot spectrometer for airglow studies. *Journal of Physics E: Scientific Instrumentation* 13:562–568.

McLandress C., Shepherd G.G., and Solheim B.H. (1996). Satellite Observations of Thermospheric Tides: Results from the WIND Imaging Interferometer on UARS. *Journal of Geophysical Research* 101: 4093–4114.

Palo S.E., Hagan M.E., Meek C.E., Vincent R.A., Burrage M.D., McLandress C., Franke S.J., Ward W.E., Clark R.R., Hoffmann P., Johnson R., Kürschner D., Manson A.H., Murphy D., Nakamura T., Portnyagin Yu. I., Salah J.E., Schminder R., Singer W., Tsuda T., Virdi T.S., Zhou Q. (1997). An Intercomparison between GSWM, UARS, and Ground Based Radar Observations: a case-study in January 1993. *Annales Geophysicae* 15: 1123–1141.

Palo S.E., Portnyagin Y.I., Forbes J.M., Makarov N.A., and Merzlyakov E.G. (1998). Transient Eastward-propagating long-period waves observed over South Pole. *Annales Geophysicae* 16: 1486–1500.

Portnyagin Y.I., Forbes J.M., Makarov N.A., Merzlyakov E.G. and Palo S.E. (1998). The summertime 12-h wind oscillation with zonal wavenumber  $s=1$  in the lower thermosphere over the South Pole. *Annales Geophysicae* 16: 828–837.

Phillips A. and Vincent R.A. (1989). Radar Observations of Prevailing Winds and Waves in the Southern Hemisphere Mesosphere and Lower Thermosphere. *PAGEOPH* 130: 303–318.

Sivjee G.G. and Walterscheid R.L. (1994). Six-hour zonally symmetric tidal oscillations of the winter mesopause over the South Pole Station. *Planetary and Space Science* 42: 447–453.

Vincent R.A. (1994). Gravity-wave motions in the mesosphere and lower thermosphere observed at Mawson, Antarctica. *Journal of Atmospheric and Terrestrial Physics* 56: 593–602.

Yudin V.A., Khattatov B.V., Geller M.A., Ortland D.A., McLandress C., Shepherd G.G. Thermal Tides and Studies to tune the Mechanistic Tidal Model using UARS Observations. *Annales Geophysicae* 15: 1205–1220.